

Dynamics of Footbridges through Operational Modal Analysis and Vibration Control using Tuned Mass Dampers

Gidewon G. Tekeste

'Department of Civil Engineering, Architecture and Georresources, Instituto Superior Tecnico, University of Lisbon, Portugal'

Abstract

This paper focuses on the implementation operational modal analysis (OMA) technique applied to pedestrian bridges with the aim of studying its dynamics, and controlling vertical and lateral vibrations induced by pedestrians by providing energy absorbers (Tuned mass Dampers) during which the pedestrian traffic frequency matches the natural frequency of the structure. The actual modal parameters during service conditions are necessary in designing the properties of Tuned Mass Dampers for effective operation. Ambient vibration tests carried out on a steel footbridge owned by Energias de Portugal (EDP) made it possible to extract its modal parameters using Enhanced Frequency Domain Decomposition method programmed in MATLAB and cross-checked against the modal estimates of standard ARTeMIS v.3.6. The compliance of mode shapes obtained using FEM method and OMA reveals the classic stiffer estimation of OMA, and probable reasons of other related results are discussed. Numerical simulation of footbridge aiming at measuring the extent of TMDs efficiency in controlling vibration due to resonance of pedestrian frequencies under worst traffic scenario yielded satisfactory results ranging up to 50% of reduction on the responses measured without TMDs, and thus making it less prone for vibration issues for serviceability conditions. FEM updating using OMA modal parameters extracted was also performed by modelling the glass panel housing the footbridge and modelling additional rotational springs at supports to simulate certain fixity of end supports observed in mode shape from ambient vibration tests. Updated model vibration levels are then investigated for serviceability comfort level criteria.

1. Introduction

The development of the output only analysis or operational modal analysis in the past two decades has brought a new attention to the study of vibration induced effects in different civil engineering structures, including slender footbridges, without the need of artificial excitation source. Within the wider research in the field of dynamic behavior of structures using ambient excitation source, the vibration control with respect to ultimate and serviceability limit states – especially under resonant conditions in different directions – has consequently gained a new interest.

Ambient modal identification, also known as Operational Modal Analysis (OMA), aims at identifying the modal properties of a structure based on ambient vibration data collected when the structure is under its operating conditions, i.e., no initial excitation or known artificial excitation. Generally, OMA methods can be classified in two types: One of them comprehends the operational modal analysis methods used to process data from ambient vibration tests. Another one involves the long-term automated operational modal analysis methods, used to process continuous dynamic monitoring signals from data acquisition system.

In ambient vibration tests, the structural ambient response is captured by one or more reference sensors at fixed positions, together with a set of roving sensors placed at different measurement points along the structure in different setups. The collected structural response is processed by two main groups of operational modal identification methods, namely non-parametric and parametric methods in both frequency and time domains.

In early 1990s, the Natural Excitation Technique (NExT) was proposed by James [2]. It is a significant breakthrough for modal identification, because only output measurements in the case of natural excitation are used for modal parameters estimation. The underlying principle of the NExT technique is that correlation functions (COR) between the responses can be expressed as a sum of decaying sinusoids. A method was evolved named as Covariance driven Stochastic Subspace Identification (SSI-COV) method by Peeters in 2000[4] based on NExT. Similarly, in frequency domain, output spectra can be modeled in a similar way as FRFs under the assumption that the input is white noise. By replacing the FRFs matrix with the output spectral matrix, the traditional CMIF method and p-LSCF procedure evolved to frequency domain decomposition (FDD) method which is shown by Brincker et al [5] in the year of 2001.

At the same time, in the 1990's, stochastic subspace identification (SSI) technique was developed in control engineering by the leadership of Van Overschee in 1996 [6]. It starts by projecting the row space of the 'future' outputs

into the row space of ‘past’ outputs, factorization of the projecting matrix leading to Kalman filter state sequence, which can be utilized to estimate system matrix by least square (LS) techniques and is named as SSI-DATA by Peeters[7].

Pedestrian traffic modelling was a discipline which gained knowledge mainly after the vibration problem which occurred on Millennium Bridge in 2000, leading to its closure, during the inauguration ceremony. Detailed research studies, e.g. Pat Dallard [8], on Millennium Bridge revealed the lateral lock-in effect and opened an era for pedestrian induced vibration problems. Before several studies have been done on load models .e.g.Bachmann [9]. He proposed some Fourier constants that should be adopted for simulating pedestrians with harmonic load for the orthogonal directions of movement and for various patterns of movement .Later, several advanced studies was done as the subject requires complex human psychological effect embedded into it. Among the researches done, SYNPEX Guidelines [10] provides detailed Fourier coefficients and phase angles for various directions and movement patterns. Load models for group of pedestrians classified in to different classes was also studied by SYNPEX. Design Guidelines to limit vibration problems had been devised by setting several classes of comfort by Christoph Heinemeyer [11] and others in 2009.

In the field of vibration control, it should be stressed that several systems have been used in the past aiming to reduce the dynamic responses of structures to desired values. These systems are frequently classified by their type of control as active, passive, semi-active and hybrid systems. The passive TMD device consists in a vibration absorber system with roots on Frahm’s vibration absorber [1]. A passive TMD is usually composed by a secondary mass suspended through a parallel assembly of a viscous damper and a spring from the primary structure, tuned to a particular structural frequency. If correctly tuned, when excited, the device will resonate out of phase with the footbridge motion, leading to a reduction of the vibration level of the primary structure under various levels of pedestrian traffic .Use of TMD for pedestrian induced vibration was studied by Caetano, E. Cunha, A. Moutinho and C. Magalhães [13] & [14].

2. Theoretical Background

The core assumption of OMA is that the excitation force is a flat spectrum white noise, characterized by a zero mean, and a time-invariant system which are the basis for the development of mathematical models for estimation.

2.1. Equation of motion of a Structure

The dynamic behaviour of a mechanical system can be often idealized by discretizing in n_m masses connected by springs and dampers (DOFs), the corresponding motion being described by the following matrix differential equation

$$M\ddot{q}(t) + C_2\dot{q}(t) + Kq(t) = f(t) = B_l u(t) \quad (1)$$

Where $M, C_2, K \in \mathbb{R}^{n_m \times n_m}$ are the mass, damping and stiffness matrices; $\ddot{q}(t), \dot{q}(t), q(t) \in \mathbb{R}^{n_m}$ are displacement, velocity and acceleration vectors at continuous time t , respectively; $f(t) \in \mathbb{R}^{n_m}$ is the excitation force vector, which can be factorized into a matrix $B_l \in \mathbb{R}^{n_m}$ specifying the locations of inputs and an input vector $u(t) \in \mathbb{R}^{n_m}$. In a practical modal experiment, output measurements are only a set of responses measured from well selected points, and not all n_m DOFs described in FE model.

2.2. Transfer Function

Assuming a viscous damping, the solution to equation of motion can be obtained as transfer function in PFE (Partial Fraction Expansion) using Fourier transform

$$H(j\omega) = \sum_{i=1}^{n_m} \left(\frac{R_{ri}}{s-\lambda_i} + \frac{R_{ri}^*}{s-\lambda_i^*} \right) \quad (2)$$

$$H(j\omega) = \sum_{i=1}^{n_{re}} \left(\frac{R_i}{j\omega-\lambda_i} + \frac{R_i^*}{j\omega-\lambda_i^*} \right) + \sum_{i=1}^{n_m} \left(\frac{R_i}{j\omega-\lambda_i} + \frac{R_i^*}{j\omega-\lambda_i^*} \right) \quad (3)$$

In classical modal analysis, λ_i, λ_i^* are named as system poles, and ϕ_i, γ_i and R_{ri} are defined as mode shape vector, mode participation vector and residue, respectively. If n_{re} is the number of retained modes Eq. (3) reduce to

$$H(j\omega) = \sum_{i=1}^{n_{re}} \left(\frac{R_i}{j\omega-\lambda_i} + \frac{R_i^*}{j\omega-\lambda_i^*} \right) \quad (4)$$

The modal reduction is then a step closer to real experimental world and basis for Frequency domain identification methods.

2.3. Peak picking and Enhanced Frequency Domain Decomposition (EFDD)

In OMA, the relation between the constant input spectrum S_{con} and the output spectrum S_{yy} can be expressed as [22]

$$S_{yy}^+(j\omega) = H(j\omega)S_{con}H(j\omega)^H \quad (5)$$

Where $S_{yy}^+(j\omega) \in \mathbb{C}^{l \times l}$ and $S_{con} \in \mathbb{C}^{m \times m}$ are the power spectra matrices of the output and input measurements, and l, m are the number of output and input responses. $H(j\omega) \in \mathbb{C}^{l \times m}$ is the FRF matrix. The superscript $(\cdot)^H$ denotes complex conjugate and transpose.

Peak picking is the simplest frequency domain estimation method that assumes spectrum around ω_i is dominated by a single mode. The counter part of Eq. (5) in time domain, correlation matrix, can be decomposed into partial fractions and considering the first two terms which correspond to positive time lag leading to two positive poles.

$$S_{yy}^+(j\omega) = \sum_{i=1}^{n_r} \frac{\phi_i g_i^T}{j\omega - \lambda_i} + \frac{\phi_i^* g_i^H}{j\omega - \lambda_i^*} \quad (6)$$

Thus peak picking starts by defining a scalar constant $\alpha_i = -\frac{d_i}{\xi_i \omega_i}$ and at resonance,

$$S_{yy}(j\omega) \approx \alpha_i \phi_i \phi_i^T \quad (7)$$

The implementation of the Peak-Picking method was firstly developed by Felber [25]. It is suggested to consider the averaged normalized power spectrum density (ANPSD) of all measured locations, which means the diagonal elements of the spectrum matrix $S_{yy}^+(j\omega)$. In case of peak-picking due to the lack of validation criteria, coherence of records can be used as its value goes close to unity around the natural frequencies of the structure.

The assumption of this method is that damping is low and the modes are well-separated, violation of these

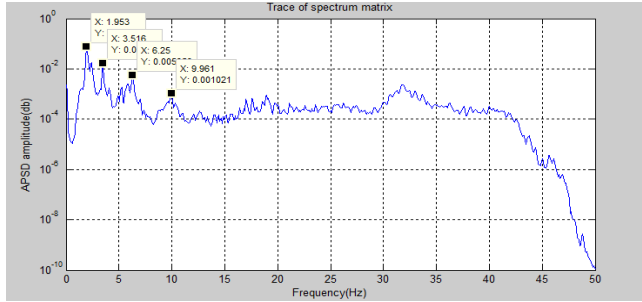


Figure 1-Trace of spectrum (ANPSD) e during construction

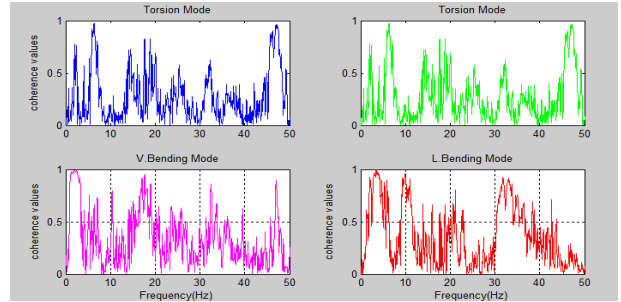


Figure 2-Coherence plots among various channels for EDP's Footbridge during construction

assumptions leads to erroneous results. Instead of identifying mode shapes, only operational deflection shapes (ODS) can be determined. In order to overcome these drawbacks of peak-picking method, a more advanced procedure named Frequency Domain Decomposition (FDD) was developed as an alternative.

The key step of FDD method is Singular Value Decomposition (SVD) of the spectra matrix at each discrete frequency ω_i . It is also interpreted in modal analysis that the FRF or spectrum matrix evaluated at a certain frequency is only determined by a few modes, and the number of these modes coincides with the rank of the spectrum matrix. It was developed to estimate modal parameters in OMA by Brinker [5]. The first step in this method is also estimation of half power spectra.

$$y(t) = [\Phi] q(t) \quad (8)$$

Using Eq. (8) in the expression of the correlation matrix of the responses we get

$$[C_{yy}(\tau)] = E\{y(t+\tau)y^T(t)\} = E\{[\Phi] q(t+\tau)[\Phi]^H q^H(t)\} = [\Phi] C_{qq}(\tau) [\Phi]^H \quad (9)$$

Applying the Fourier transform to Eq. (9) gives

$$S_{yy}(j\omega) = [\Phi] G_{qq}(j\omega) [\Phi]^H \quad (10)$$

Then, by taking the SVD of $S_{yy}^+(j\omega)$ at each discrete frequency ω_i it can be decomposed as follows

$$S_{yy}^+(j\omega_i) = U(\omega_i) S(\omega_i) U^H(\omega_i) \quad (11)$$

Where $S(\omega_i)$ is a diagonal matrix holding the singular values sorted in descending order $S(\omega_{ij}), j = 1, 2, \dots, l$, $U(\omega_i) = [u_1(j\omega_i), u_2(j\omega_i), \dots, u_l(j\omega_i)]$ is a unitary matrix holding the singular vectors (columns of U) $u_j(j\omega_i)$. When the frequency approaches a certain resonance frequency ω_r , the power spectra matrix can be approximately decomposed as a rank one matrix. If only one mode is dominating at the resonance frequency ω_r , the corresponding singular vector $u_1(\omega_r)$ is an estimate of the corresponding mode shape with unitary normalization.

$$\hat{\phi}_r = u_1(\omega_r) \quad (12)$$

Mode shapes can be obtained from the corresponding singular vectors assuming the mode shapes are orthogonal. Because SVD has the ability to separate the signal space from noise space, the modes can be indicated from singular value plots with noisy measurements, and closely spaced modes or even modes with repeated modal frequencies can be easily detected. Nevertheless, modes obtained are unscaled.

MAC (Modal Assurance Criterion) value is computed between the SDOF singular value at resonance and the singular values of frequency lines centered at this resonance frequency as [5]

$$MAC_i = \frac{(\hat{\phi}_r \phi_i^T)^2}{(\hat{\phi}_r \phi_i^T)(\hat{\phi}_r^T \phi_i)} \quad (13)$$

If a singular vector ϕ_i is found to have high MAC value (a user defined value, commonly 0.8 as a starting value), with $\hat{\phi}_r$, the corresponding singular value is included in the definition of the SDOF auto spectra function. In addition, mode complexity factor can be used for validation of individual modes given by

$$MCF_i = 1 - \frac{(S_{yy} - S_{xx})^2 + 4S_{xy}^2}{(S_{yy} + S_{xx})^2} \quad (14)$$

Where $S_{xx} = Re\{\phi_i\}^T Re\{\phi_i\}$, $S_{yy} = Im\{\phi_i\}^T Im\{\phi_i\}$, and $S_{xy} = Re\{\phi_i\}^T Im\{\phi_i\}$

The Later distinguishes real mode (0 value) and imaginary mode (1 value) and is given in percentage. From the fully or partially identified SDOF auto spectra function, an approximation of the correlation function of the SDOF system is obtained by taking the spectral density function back to time domain by inverse FFT. From this free decay function in time domain (the correlation function of the SDOF system), the natural frequency and the damping is found by estimating crossing times and logarithmic decrement. Firstly, all peaks r_{pk} on the correlation function are found. The logarithmic decrement δ_k at kth frequency is calculated as

$$\delta_k = \frac{1}{p} \ln\left(\frac{r_{0k}}{|r_{pk}|}\right) \quad (15)$$

Where r_{0k} the initial peak value of the correlation function and r_{pk} is the pth peak at the kth mode. In order to reduce noise from the correlation function normalized peak values between 0.95-0.3 are used in this project,

$$\xi_k = \frac{\delta_k}{\sqrt{\delta_k + 4\pi^2}} \quad (16)$$

The damped natural frequency ω_{dk} is found by making a linear regression between the crossing times and the times corresponding to the peaks. The natural frequency ω is found by

$$\omega_k = \frac{\omega_{dk}}{\sqrt{1 - \xi_k^2}} \quad (17)$$

The Fully developed EFDD MATLAB program was used for the ambient vibration records modal estimation and its application is presented.

2.4. Time Domain Models, Stochastic sub-space identification methods

These models reveal the inherent relation between modal model of vibration systems and output measurements without converting from the signals to frequency domain, the modal parameters can be fitted directly from time series analysis (TSA) based on parametric models. The modal identification results estimated by these models in time domain can be correlated with the results produced by frequency domain models. It is worth to identify the main disparity between the two approaches (time domain and frequency domain) in order to reach a conclusion on the effectiveness of each methodology. The second order vibration equation in state-space form can be written as [6]

$$P\dot{x}(t) + Qx(t) = F \quad (18)$$

Where

$$P = \begin{bmatrix} C_d & M \\ M & 0 \end{bmatrix}, \quad Q = \begin{bmatrix} K & 0 \\ 0 & M \end{bmatrix}, \quad x(t) = \begin{bmatrix} q(t) \\ \lambda q(t) \end{bmatrix}, \quad F = \begin{bmatrix} B_i \\ 0 \end{bmatrix} u(t)$$

Pre-multiplying Eq. (18) by P^{-1} ,

$$\dot{x}(t) = A_c x(t) + B_c u(t) \quad (19)$$

Where the sub index 'c' denotes continuous time, $A_c \in \mathbb{R}^{n \times n}$ is the state matrix and $B_c \in \mathbb{R}^{n \times n}$ is the input matrix. They are given by

$$A_c = P^{-1}Q = \begin{bmatrix} C_d & M \\ M & 0 \end{bmatrix}^{-1} \begin{bmatrix} K & 0 \\ 0 & M \end{bmatrix} = \begin{bmatrix} 0 & I \\ -M^{-1}K & -M^{-1}C \end{bmatrix}, \quad B_c = P^{-1} \begin{pmatrix} B_i \\ 0 \end{pmatrix} = \begin{bmatrix} 0 \\ M^{-1}S \end{bmatrix}$$

Where the sub index 'c' denotes continuous time, $C_c \in \mathbb{R}^{l \times n}$ is the output matrix and $D_c \in \mathbb{R}^{l \times n}$ is the direct transmission matrix. Using the second order equation of motion and the definition of the state vector $x(t)$ in Eq. (19), the observation Eq. (40) can be expressed as

$$y(t) = C_c x(t) + D_c u(t) \quad (20)$$

C_c and D_c are given by

$$C_c = [-C_a M^{-1}K \quad C_v - C_a M^{-1}C_2], \quad D_c = C_a M^{-1}B_i \quad (21)$$

Combining Eqs. (19) and (20), the classical continuous-time state-space (SS) model is given by

$$\dot{y}(t) = C_c x(t) + D_c u(t), \quad \dot{x}(t) = A_c x(t) + B_c u(t) \quad (22)$$

In this study, Data driven SSI was discovered for its preliminary use in identification of model order of the system. The detailed derivation of estimation system matrices will not be presented here, a detailed derivation of various SSI algorithms are available [4]. The initial step in SSI method is to divide the record as past and future matrix and formation of Hankel matrix followed by projection of row space of future outputs on to row space of past outputs to form projection matrix, may be computed by RQ factorization. MATLAB based program developed was developed to estimate the model order. Nevertheless stabilization diagram was not dealt due to poor speed efficiency of the program. Model of the aforementioned records exhibit a drop between 2 and 3 model order which indicates only two singular values are important on the estimation of the modal parameters.

2.5. Pedestrian Traffic as source of excitation

During normal walking, the vertical forces are centered at a frequency in the range of 1.2Hz - 2.3 Hz (lower range represent the 5% slow and upper range represent 95% fast, SYNPEX[13]) corresponding to the pace rate. For running the frequencies lie in the range 2Hz – 3.5Hz. In the other hand, lateral forces fall in the frequency range 0.5Hz-1.2Hz (half of the vertical frequency) with a minimum of 0.5Hz, attained from a recommendation of Millennium Bridge which caused Lock-in effect. Synchronization between bridge and pedestrians may cause Lateral Lock-in effect Known as synchronous Lateral excitation (SLE).

Vertical walking forces due to human footsteps can be divided into different periodic oscillations by a Fourier transformation,

$$F(t) = F_0 + \sum_i F_i \sin(2\pi f_s t - \varphi_i) = G(1 + a_1 \sin(2\pi f_s t - \varphi_1) + a_2 \sin(4\pi f_s t - \varphi_2) + \dots \quad (23)$$

Where F_0 -Mean or static load (person's weight), F_i -Load component for frequency f_s , f_s -Human step frequency and φ_i -Phase angle of the load component F_i

The Fourier coefficients proposed by several authors show a large scatter mainly due to person psychological differences and uncertainties in measurements, e.g. Bachmann [9], and SYNPEX gives coefficients which depend on step frequency. Similarly, Horizontal force of walking pedestrian can be modelled as

$$F(t) = \sum_i F_i \sin(2\pi f_s t - \varphi_i) \quad (24)$$

Where i has the (non-whole) values of 1/2, 1, 3/2, 2, etc.

Additionally, a uniformly distributed vertical harmonic load can simulate a stream of pedestrians given by

$$p(t) = P \times \cos(2\pi f_s t) \times n' \times \psi \quad (25)$$

Where P -Force component for a pedestrian with frequency of f_s , f_s -Step frequency, assuming it to be equal to the bridge vibration mode, n' -Equivalent number of persons (depends on the 95th percentile) [25] and ψ -Reduction coefficient that takes into account the probability that the frequency of walking approaches the critical frequency range into consideration [25]

Individual person load in vertical, longitudinal and lateral are 280N, 140N and 35N respectively [25].

The serviceability checks of footbridge is done in accordance to comfort class maximum acceleration for Vertical and Horizontal direction given in the 3rd International footbridge conference [25].

2.6 Equations of a SDOF-TMD System

The governing equations of a general single degree-of-freedom (SDOF) damped system linked to a TMD, represented in Figure 3 are presented in this sub-section.

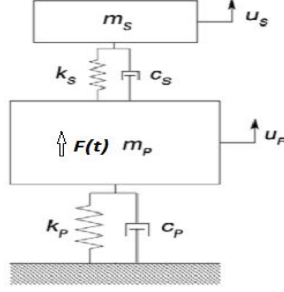


Figure 3-Scheme of a SDOF system linked to TMD

Let us denote the mass, stiffness and damping of each of the systems by m_j , k_j and c_j , where the subscript j should be equal to P or S , respectively for the primary or secondary (TMD) systems.

The governing equations of a SDOF mass, subjected to a simple harmonic excitation of frequency ω expressed by $F(t) = F_0 e^{-i\omega t}$, to which a TMD is attached, can be obtained by applying Newton's law to each of the masses that compose the system, leading to the following set of equations of motion:

$$m_p \ddot{u}_p(t) + (c_p + c_s) \dot{u}_p(t) - c_s \dot{u}_s(t) + (k_p + k_s) u_p(t) - k_s u_s(t) = F(t) \quad (26)$$

$$m_s \ddot{u}_s(t) + c_s \dot{u}_s(t) - c_s \dot{u}_p(t) + k_s u_s(t) - k_s u_p(t) = 0 \quad (27)$$

Where $u_p(t)$, $\dot{u}_p(t)$ and $\ddot{u}_p(t)$ represent the vertical displacement, velocity and acceleration of the primary mass, in the same order, $u_s(t)$, $\dot{u}_s(t)$ and $\ddot{u}_s(t)$ represent the secondary system, and the relative displacement of the TMD mass with respect to the displacement of the primary system (or TMD stroke) is defined as the difference of u_p and u_s . In the case of a linear time-invariant system, the steady-state response is given by

$$u_p = u_{po} e^{-i\omega t} \quad (28)$$

$$u_s = u_{so} e^{-i\omega t} \quad (29)$$

Hence, Eqs. (28) and (29) yield non-dimensional complex transfer functions for a harmonic excitation force referring to the displacement of the primary and secondary masses, respectively, as follows:

$$|G_P(r_p)| = \left| \frac{u_{po}}{F_0/K_P} \right| = \sqrt{\frac{(q^2 - r_p^2)^2 + (2i\xi_s q r_p)^2}{[(1 - r_p^2)(q^2 - r_p^2) - \mu r_p^2 q^2 - 4\xi_s \xi_p q r_p^2]^2 + 4r_p^2 \{\xi_p (q_s^2 - r_p^2) + \xi_s q [1 - r_p^2 (1 + \mu)]\}^2}} \quad (30)$$

$$|G_S(r_p)| = \left| \frac{u_{so}}{F_0/K_P} \right| = \sqrt{\frac{q^4 + (2i\xi_s q r_p)^2}{[(1 - r_p^2)(q^2 - r_p^2) - \mu r_p^2 q^2 - 4\xi_s \xi_p q r_p^2]^2 + 4r_p^2 \{\xi_p (q_s^2 - r_p^2) + \xi_s q [1 - r_p^2 (1 + \mu)]\}^2}} \quad (31)$$

Where the natural frequency of the primary and secondary systems are denoted as $\omega_p = \sqrt{k_p/m_p}$ and $\omega_s = \sqrt{k_s/m_s}$ respectively, TMD mass to primary mass ratio, $\mu = m_s/m_p$, and the damping ratios for the primary and secondary systems as $\xi_p = c_p/(2m_p\omega_p)$ and $\xi_s = c_s/(2m_s\omega_s)$, respectively, $r_p = \omega/\omega_p$ and $q = \omega_s/\omega_p$.

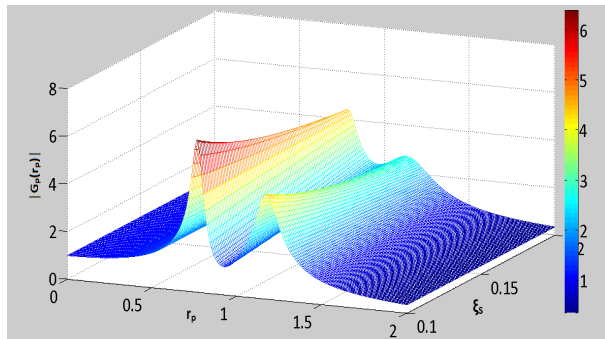


Figure 4-Displacement transfer function plot at $q=0.9$ and $\mu=0.2$

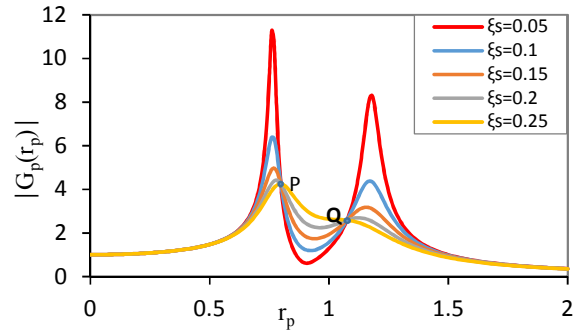


Figure 5-Displacement transfer function plot at $q=0.9$ for various ξ_s

2.7 Dynamic Control through TMDs

In order to tune the TMD, i.e. find out the optimal values for mass, damping and stiffness of the TMD, several criteria may be chosen. Since for pedestrian traffic, the excitation can be associated to a periodical distributed loading, leading to narrow banded excitation frequencies (usually 0.5-4.6Hz), to achieve good performance it is recommended to minimize the maximum of the transfer function, rather than its area. With this purpose, one possibility is to use the well-known Den Hartog [15] optimal criterion, valid for primary systems with vanishing damping,

$$q_{opt} = \frac{1}{1+\mu} \quad (32)$$

$$\xi_{opt} = \sqrt{\frac{3\mu}{8(1+\mu)}} \quad (33)$$

where q_{OPT} and ξ_{OPT} denote the optimal frequency and damping ratio. These expressions give an excellent prediction to the optimal TMD parameters for cases when the external excitation is mainly periodic and the damping of the primary system is low as with the case of steel footbridges. Therefore, in the numerical optimization procedure only the frequency ratio q and the damping ratio ξ_s are computed for each of the chosen set of mass ratios. The relative displacement of the TMDs, given in Eq. 34, is also an important aspect due to limited space of room for TMD movement in the case study. The increase in mass of TMD results in reduction of this parameter, but with the predefined mass ratio for the factors aforementioned, the optimal damping for TMD in order to reduce relative displacement was performed in the MATLAB Min-max optimization program.

$$|G_r(r_p)| = \left| \frac{u_r}{F_0/K_p} \right| = \sqrt{\frac{q^4}{[(1-r_p^2)(q^2-r_p^2)-\mu r_p^2 q^2 - 4\xi_s \xi_p q r_p^2]^2 + 4r_p^2 \{ \xi_p (q_s^2 - r_p^2) + \xi_s q [1 - r_p^2(1+\mu)] \}^2}} \quad (34)$$

Den Hartog's undamped structure optimization criteria converges to numerically optimized solution, programmed in MATLAB for non-vanishing damping, in the range of 1-5% structure damping. Thus it can be concluded that Den Hartog criteria can be only applicable for structures whose damping values are in the range 1-5%. And the method is best fitted for small mass ratios, practical, in terms of optimized parameters,

3. Operational Modal Analysis of EDP's Footbridge

3.1. Footbridge description

EDP (Energias de Portugal), which is the electric supplying company in Portugal, recently built a composite structure building in Cais do Sodre, Lisbon. The new building have two compartment buildings parallel to each other on the east-west direction and connected by two slender housed steel footbridges with aesthetically appealing glass panels. Due to the similarity of the footbridges in terms of geometry, location and excitation forces, the North footbridge is chosen as a case study to be investigated. The footbridges are also decided to be equipped with TMDs in an effort to control pedestrian induced vibrations.

The footbridge spans 49.87m, simply supported, at the opposite facing buildings in its bottom part, at both ends and also the roof is supported to one of the building at one end of the footbridge. The footbridge has 2.925m width and is laterally supported by less stiff ceramic finished steel welded plates to the west side.

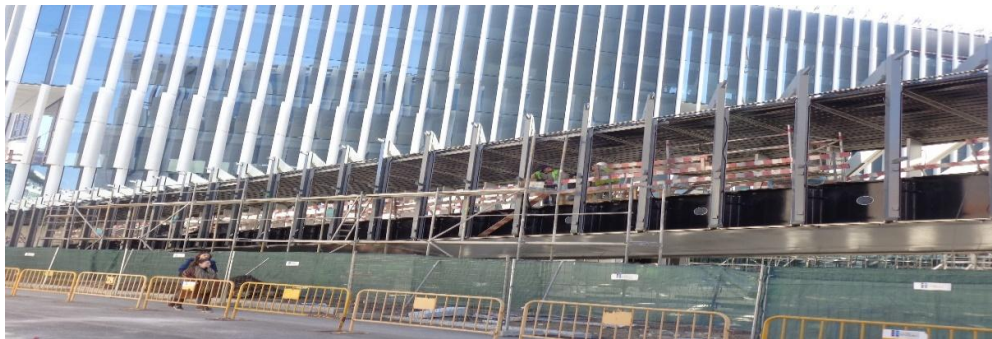


Figure 6-North Footbridge of EDP's Building, Cais do Sodre, Lisbon

The footbridge has a central plate girder inside a trapezoidal hollow metal box which tapers as the bridge descends. The deck is a steel plate; housed by glass panels; roof built up with rectangular hollow sections and braced by square hollow sections. The TMDs are housed in the steel box deck as shown in Figure 7.

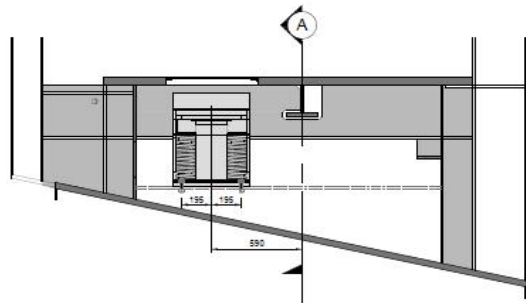


Figure 7-Mid-span cross section with TMD

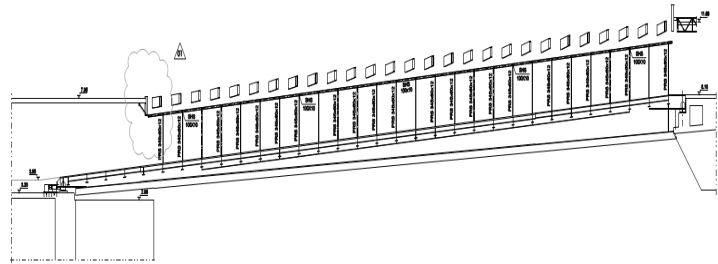


Figure 8-North Footbridge side view

Table 1-TMD Parameters

TMD units	Mass[kg]	K[N/m]	C[Ns/m]	f[Hz]	Amplitude[mm]
2	1241	55948	1401	1.07	120

In this research, Two Etna tri-axial accelerometers were used for collecting the ambient vibration records, triggered through PC with a Kinematics Quick Talk software capable of adjusting sensor parameters and triggering, during the construction stage of the footbridge. After completion of construction process, 2 sets of 3 uni-axial accelerometers, three being mounted in one location, are used by taking advantage of the structural health monitoring data acquisition system. Sensor layout for data acquisition is planned as shown in Figure 9.

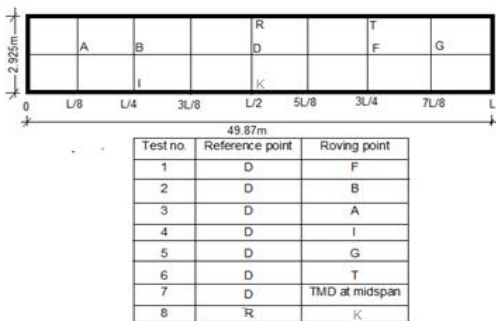


Figure 9-Sensor layout for two point setup

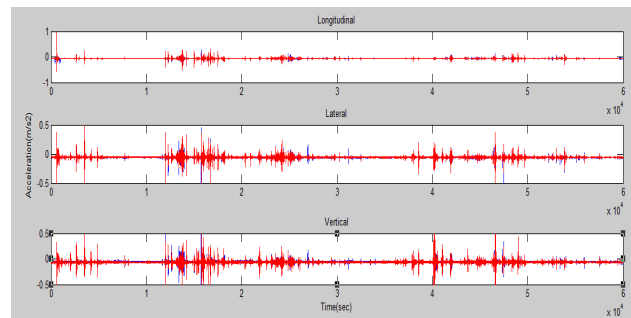


Figure 10-Six channels of acceleration record at Mid-span

3.2. Signal conditioning

The choice of Nyquist Frequency, 100Hz, is sufficient enough to avoid effects of aliasing error, but during decimation process to reduce the sampling frequency, possible alias is treated by anti-aliasing low pass Chebysev Type I IIR filter of order 8. Application of windowing to reduce leakage of peak spectral values around resonance to adjoining frequency lines using Hann window and followed by detrending of data to reduce any linear trend in the data or mean value.

3.3. Modal estimation using Enhanced Frequency Domain Decomposition Method

Due the mass and stiffness discrepancy before and after completion, the need, for comparison of modal parameters is not recommended, but note should be taken that less stiffer modes after completion are associated to increased mass for a fairly constant stiffness. Thus, next results dialog only in the later records.

The noise introduced in to the estimation is investigated by the profile of peak values of the normalized correlation function and 0.9 MAC criteria is adopted, recommended for noisy or less reliable data.

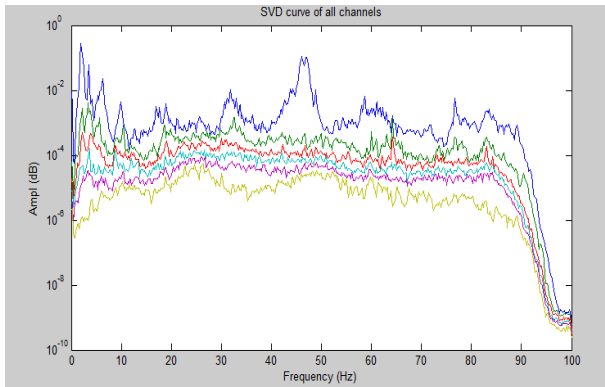


Figure 11. Singular value plot before completion

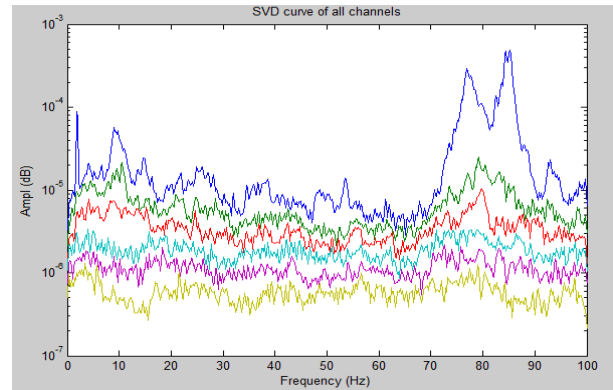


Figure 12. Singular value plot after completion

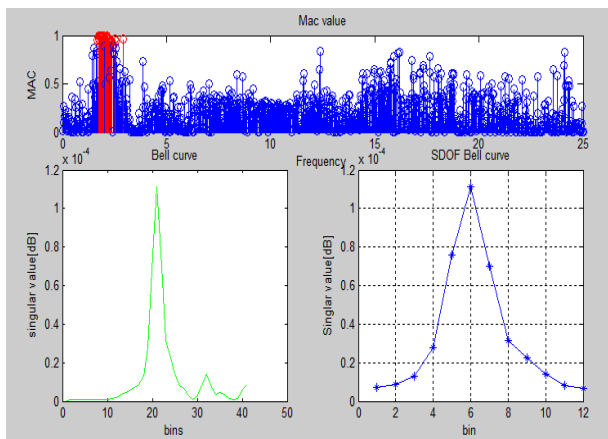


Figure 13. MAC value across frequency line and SDOF bell curve-1st V mode

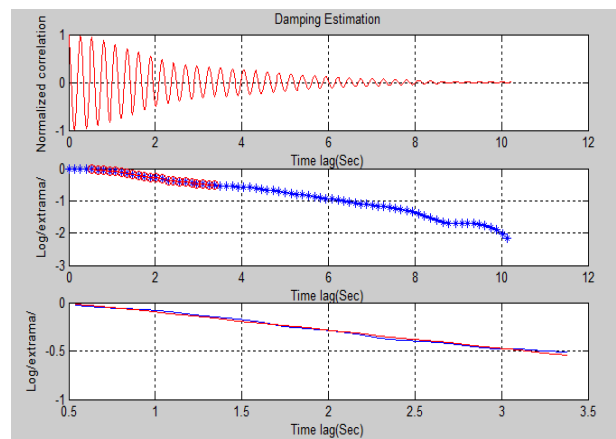


Figure 14. Damping estimation from Free decay plot using curve fitting-1st V mode

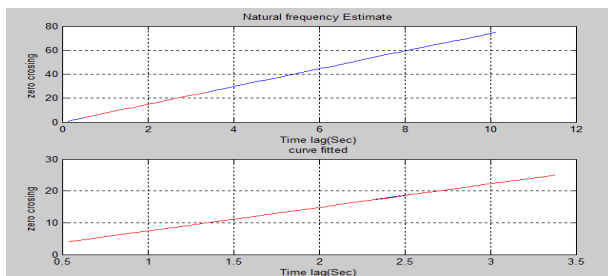


Figure 15-Zero crossing for Natural frequency estimation -1st V mode

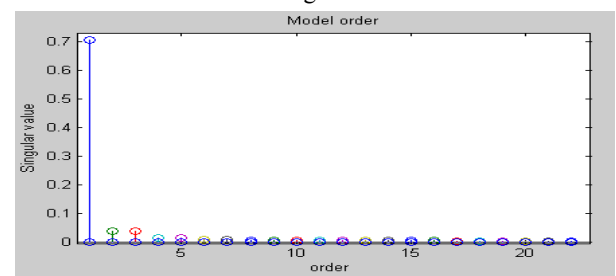


Figure 16-SSI-DATA Model order after completion

Frequency domain method of modal estimation program written in MATLAB was employed to determine the modal parameters. All setups are used one after the other, and mode shapes resulted from all the setups is computed using the reference sensor mode shape ratio factor [26] and 4 modes are extracted. ARTEMIS standard version 6 is used also for comparison of results obtained from the MATLAB based program. The MAC validation done among the modal estimates of same method allows to discern modes of the same shape and MAC validation among different methods gives the confidence on the modes of vibration picked (curve fitted frequency domain decomposition is considered).

Table 2. OMA vs. FEM estimated modes [V-Vertical, T-Transversal and Tor-Torsional]

Mode	FEM				OMA			Complexity (%)
	Freq. (Hz)	Mode Description	Modal Participation	Freq. (Hz)	Mode Description	Damping (%)		
						ARTEMIS	MATLAB	
1	1.09	1 ST V	0.814-Z	1.86	1 ST V	2.768	2.334	0.69
2	1.66	1 ST T	0.79-Y	-	-	-	-	-
3	3.28	2 ND V	0.021-Z	-	-	-	-	-
4	3.38	2 ND Tor	0.02-Z	3.49	1 ST L	2.726	2.706	12.18
5	3.6	1 st L+1 ST Tor	0.32-Z/0.01-Y	-	-	-	-	-
6	3.95	2 ND L+2 ND V	0.32-Z	-	-	-	-	-
7	4.71	2 ND L+2 ND V	0.01-Z/0.15-Y	-	-	-	-	-
8	9.66	4 TH V+2 ND L	0.11-Z	9.78	2 ND L+2 ND V	6.124	4.86	11.309
9	-	-	-	76.84	Local-Mid span	1.316	1.650	4.514
10	-	-	-	82.49*	Local-L/4 span	0.577	0.532	3.621

*ARTEMIS Freq., MATLAB Freq. is 85.12Hz

The first fundamental mode is characterized with high modal damping of 2.768%. This phenomena could be due to increased number of joints and non-structural elements in the footbridge. Similarly, second mode, lateral mode of vibration, presents high modal damping value and a minimal degree of 1st torsion mode. Third mode is blended mode characterized by very high damping which is exceptional for a steel footbridge as it can be manifested in the SVD plot. And higher modes obtained are local modes of vibration in the main structure and/or mode for the roof assembly. As shown in Table 2. 2nd and 3rd modes of vibration shows higher degree of complexity. Also, FEM estimated modes are compared against ambient vibration modes aiming at validation of modes of vibration and FEM model updating

Figure 17 shows the MAC validation done using ARTEMIS and mode of vibration at 9.65Hz has significant MAC value with mode shape at 76.84Hz even though modes are well separated. This could be attributed to the instrumentation done, which was not able to cover all points in the footbridge and hence those modes may have similar shapes at points of instrumentation but different shapes at non-instrumented points. Modes shapes orthogonality, i.e. independent modes, is verified if MAC values computed among modes considered is close to zero. Computed complexity values are also investigated during which modes are picked manually.

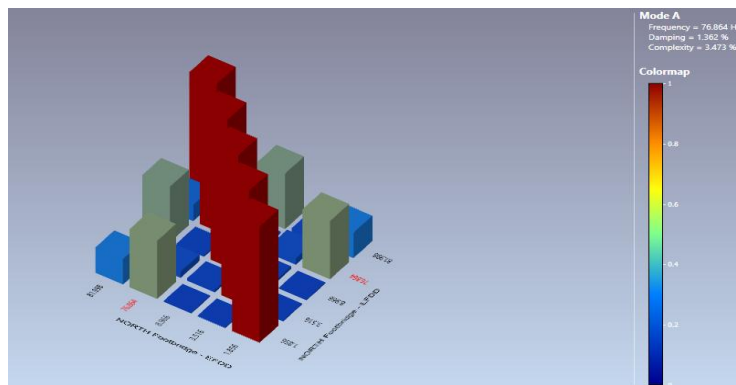
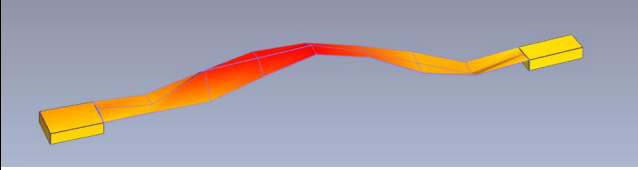
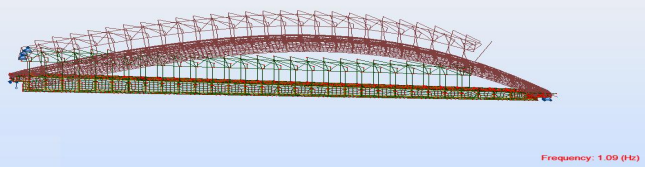
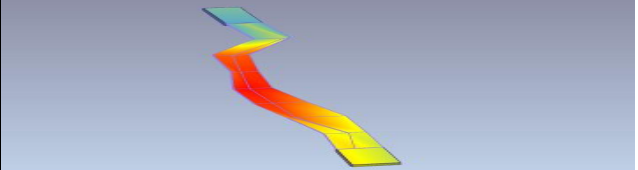
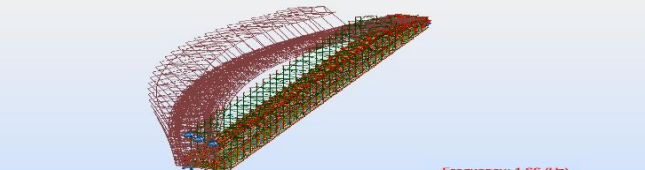
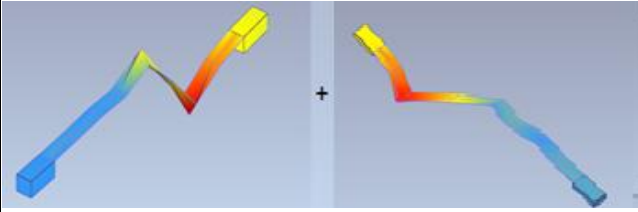
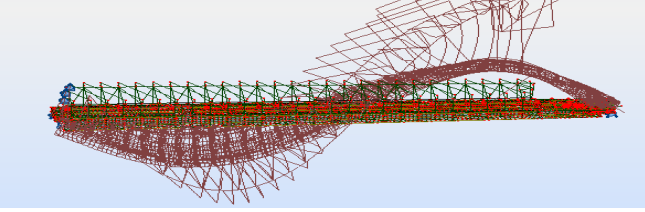
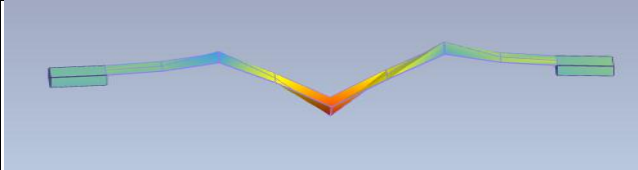
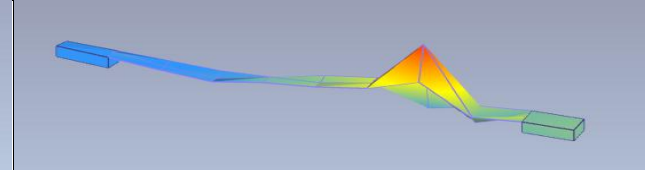


Figure. 17 MAC validation of EFDD estimates in ARTEMIS

Figure 18. Mode shapes (OMA vs. FEM)

	
OMA	FEM
1.86Hz(1 st Vertical Mode)	1.09Hz(1 st Vertical Mode)
	
OMA	FEM
3.49Hz(1 st Transversal Mode)	1.66Hz(1 st Lateral Mode)
	
OMA	FEM
9.78Hz(2 nd Vertical e+2 nd Transversal Mode)	4.71Hz(2 nd Vertical e+2 nd Transversal Mode)
	
OMA	OMA
76.84Hz(Local Mode, Mid span)	82.15Hz(Local Mode, Quarter span)

Fundamental mode shape computation in OMA resulted in stiffer estimation with an error of 41.39% and error is more pronounced in case of the 2nd lateral mode of vibration. Finite element updating is performed on the structure to allow to simulate the actual in-situ behavior of the footbridge. Modelling of glass panel stiffness with equivalent thick shell in SAP2000 with properties obtained from institute of Structural Engineering (ICE) [27] enabled the fundamental vertical mode to increase from 1.09Hz to 1.6148Hz yielding 13.18% error from the ambient vibration results. With regard to support conditions, the footbridge exhibits certain degree of fixity at supports as it can be depicted from the 1st mode shape in ambient vibration tests. Hence, rotational stiffness springs with 275,000KNm/rad (3% of fixity

moment), in U2 direction, at the 4 end supports are defined to simulate ambient modal estimate. It should be noted here, ignored are all other causes of estimation bias factors both in the FEM model and ambient vibration, the probable unmodeled stiffness of the supports is computed by determining the rotational stiffness at supports which updates the model to the ambient vibration estimate.

3.4. TMD efficiency and Serviceability check for vibration levels

Pedestrian load defined in section 2.6 is defined in SAP2000 considering the worst case scenario, i.e. Traffic class 5 with a pedestrian density of $1.5P/m^2$, as a time history load with same period as that of the fundamental vertical frequency to check vibration levels of footbridge so as to verify the serviceability criteria of appropriate comfort level under resonance condition defined by HIVOSS [25]. Through the same model, efficiency of TMDs is also investigated.

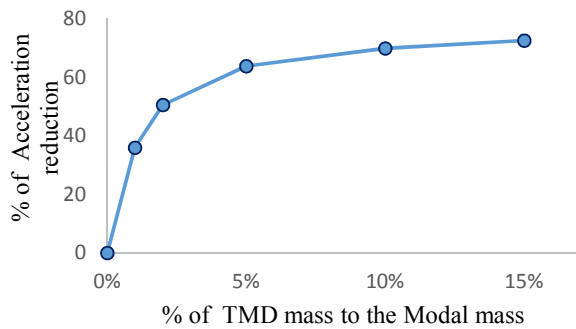


Figure 19- Percentage of maximum acceleration reduction at Mid-span due to TMD

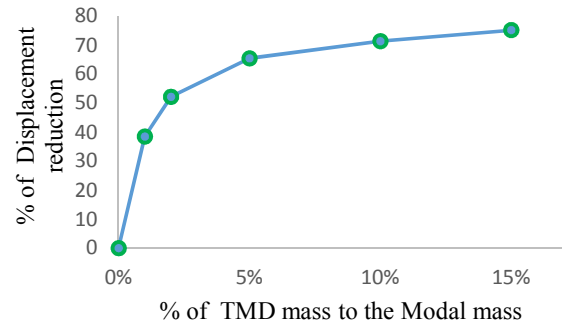


Figure 20- Percentage of maximum displacement reduction at Mid-span due to TMD

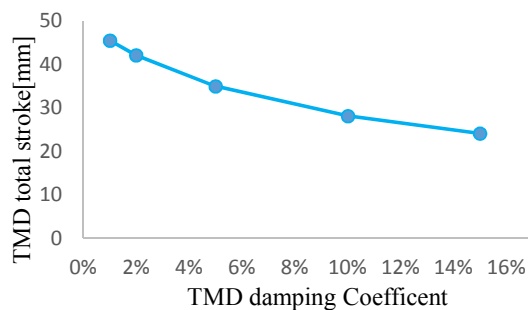


Figure 21- TMD stroke vs. damping ratio at 2% mass ratio

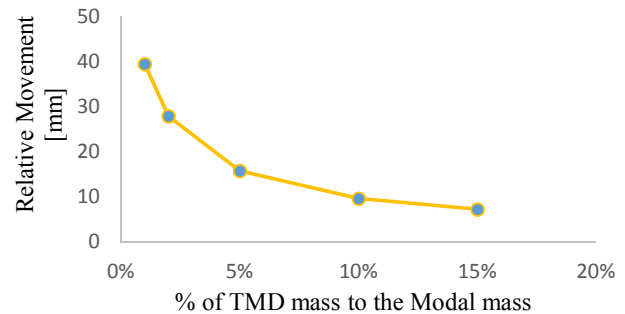


Figure 22-Relative movement vs TMD mass ratio at 2% mass ratio

Figure 19-22 shows the outcomes of the FEM analysis and it leads to a conclusion that the introduction of TMD tuned to the 1st vertical mode will significantly reduce the acceleration and displacement response of the structure more effectively at 1-5% of mass ratio and further increase in mass ratio apart from being not effective will impose structural load and increased cost. To limit the relative displacement of TMD to the available space the relative ratio of TMD mass and to the structure is found to be efficient in the same range aforementioned.

Similarly, the stroke of TMDs with varying damping of TMDs in Figure 21 indicates the efficient damping ratios of 5-10% for the available room.

To this end, the footbridge vibration level using the updated FEM model, both frequency and damping, is found to comply with the desired comfort class in vertical direction, comfort class one ($a_{max} < 0.5m/s^2$). Note: the footbridge lateral direction vibration levels are much smaller due to non-resonating action.

4. Conclusions

The present work was performed with the purpose of studying the dynamic behaviour of footbridges using operational modal analysis, determining the gap between the ambient vibration results and Finite Element Modelling solution, and finally to calibrate the vibration levels of the footbridge using the updated FEM model.

Despite the various causes of biased and erroneous results which may arise due to data acquisition noises from instrument and estimation model, external noise, harmonic signal contamination from actions in the proximity and most importantly non-compliance of excitation force with the basic assumption of OMA, operational modal analysis is proved to be a crucial tool in estimating the dynamics of footbridges and damage detection purposes. And the end of use OMA in Finite Element updating was addressed.

TMD tuning and its efficiency in suppressing pedestrian induced vibrations was also part of the study. The study made was only focused on resonance conditions i.e. when the harmonic pedestrian traffic load frequency coincides with the natural frequency of the structure to which the TMD is tuned to. The assessment of ranges of optimized values for mass ratio and damping coefficient of TMDs was performed.

The following conclusions can be drawn in relation to OMA application as:

- ❖ Unplanned and un-systematic data acquisition layout will lead to biased estimates, e.g. overlapping of close modes, and obscured modes due to spectra rank deficiency as a result of insufficient sensors
- ❖ Good choice of sampling rate and signal conditioning are very crucial especially for modal damping estimation, the need for filtering and windowing as well as spectra averaging can also be emphasized
- ❖ Good choice of MAC validation range in SDOF bell definition and proper choice of correlation ranges in the free decay function leads to better accuracy; presence of higher complexity in the observed modes should be taken carefully as it might lead to imaginary modes
- ❖ Orthogonality(independency) of modes should be checked and estimates from various approaches shall be validated

Studies done on TMD brings forward the following conclusions:

- ❖ With the increase of TMD mass ratio, the ability of this device to control vibrations of the primary structure increases. Nevertheless, this increment is more evident with mass ratios μ up to 5%;
- ❖ The TMD effectiveness is highly dependent of the frequency tuning. For the simply supported footbridge case, a variation of $\pm 10\%$ of the structural frequency for which the TMD is tuned led increase about 50% and 41.8% with respect to the response in optimal TMD case, for accelerations and displacements, respectively. Nevertheless, these response effects were still significantly lower than those without TMDs[ratio of displacements without TMD and mistuned TMD is nearly two]
- ❖ Variations on the TMD optimal damping ratio did not lead to a significant variation in the TMD effectiveness but its effect on the stroke of TMD was assessed, continuous decrement of the parameter was registered with increased mass of TMD, but become less significant if it exceeds 10%.

Acknowledgments

The research presented in this paper was carried out at the Department of Civil Engineering and Architecture (DECivil) at Instituto Superior Técnico (IST), Lisbon. The author would like to express his gratitude to Oz. Lda for making this project available for research, AFACONSULT for supplying FEM Robot model of the steel footbridge and AMIBSIG Company for assisting in data acquisition process of ambient vibration records.

References

- [1] Cunha, A.; Caetano, E.; Magalhães, F. (2007). "Output-only Dynamic Testing of Bridges and Special Structures." Structural Concrete (Fib), 8(2), 67-85.Frahm, H. (1911). "Device for Damping Vibrations of Bodies." U.S.Patent, No. 989, 958, 3576-3580.
- [2] James [1992] B. James. "Approaches to Multi-harmonic Frequency Tracking and Estimation." Australian National University Ph.D. Thesis, 1992
- [3] Akaike [1974] H. Akaike. "A New Look at the Statistical Model Identification." IEEE Transactions on Automatic Control, vol. AC-19, pp. 716-723, IEEE, 1974.
- [4] Peeters, Bart (2000). "System Identification and Damage Detection in Civil Engineering." PhD Thesis, Katholieke Universiteit Leuven, Leuven
- [5] Brincker, R.; Ventura, C.; Andersen, P. "Damping Estimation by Frequency Domain Decomposition." In Proceedings of IMAC XIX, Kissimmee, USA, 2001

- [6] Van Overschee P., De Moor B. "Subspace Identification for Linear Systems, Theory, Implementation, Applications." Kluwer Academic Publishers, (1996)
- [7] Bart Peeters and Guido De Roeck. "Reference-Based Stochastic Subspace Identification for Output-Only Modal." Mechanical Systems and Signal Processing, Volume 13, Issue 6, November 1999,
- [8] Pat Dallard, T. F. A. F. A. L. R. R. S. M. W. M. R., 2001. "London Millennium Footbridge: Pedestrian-Induced Lateral Vibration." Journal of Bridge Engineering, November/December
- [9] Bachmann, H. (1998). "Vibration Problems in Structures, Practical Guideline." Birkhäuser Verlag, Basel.
- [10] SYNPEX Guidelines. "European Project on Advanced Load Models for synchronous Pedestrian excitation and Optimized Guidelines for Design of Steel Footbridges." 2007
- [11] G. Sedlacek, Chr. Heinemeyer, Chr. Butz together with M. G eradin. "Design of Lightweight Footbridges for Human Induced Vibrations." JRC First Edition, May 2009
- [12] Frahm, H. (1911). "Device for Damping Vibrations of Bodies." U.S. Patent, No. 989, 958
- [13] Caetano, E.; Cunha, A.; Moutinho, C.; Magalh es, F. (2010b). "Studies for Controlling Human-induced Vibration at the Pedro e In es Footbridge." Portugal. Part 2: Implementation of tuned mass dampers. Engineering Structures, 32(4), 1082-1091
- [14] Moutinho, C. (1999). "Active and Passive Control of Vibrations in Footbridges." M.Sc. Thesis (in Portuguese), FEUP
- [15] J.P. Den Hartog, Mechanical Vibration, McGraw-Hill, New York, 1947.
- [16] T. Asani, O. Nishihara, A.M. Baz. "Analytical solutions to H_∞ and H_2 Optimization of Dynamic Vibration Absorber Attached to Damped Linear Systems." Journal of Vibration and Acoustics 124 (2002) 67–78
- [17] Felix Weber, Glauco Feltrin, and Olaf Huth. "F05 Guidelines for Structural Control." SAMCO Final Report, 2006
- [18] Daniel, Y. Lavan, O. and Levy, R. "Multiple-Tuned Mass Dampers for Multi-modal Control of Pedestrian Bridges." Struct. Eng., 138(9), 1173–1178., (2012)
- [19] Vanlanduit, S., Verboven, P., Guillame, P., Schoukens, J. "An Automatic Frequency Domain Modal parameter Estimation algorithm." Journal of Sound and Vibration, Vol. 265, pp. 647-661, 2003
- [20] Welch, Peter D. "The use of fast Fourier Transform for the Estimation of Power Spectra: A method based on Time Averaging over Short Modified Periodograms." IBM Watson Research Center, Yorktown Heights, N.Y., 1967
- [21] Blackman, R.B., and Tukey, J.W., 1958. "The Measurement of Power Spectra from the Point of View of Communication Engineering." Dover Publications, 190 pp.
- [22] Bendat, J.S. and Piersol, A.G. "Engineering Applications and Spectral Analysis." Wiley Interscience, New York. 1980
- [23] Cauberghe, B. (2004). "Applied Frequency-Domain System Identification in the Field of Experimental and Operational Modal Analysis." PhD Thesis, Vrije Universiteit Brussel, Belgium
- [24] Felber, A. J. (1993). "Development of a Hybrid Bridge Evaluation System." PhD Thesis, University of British Columbia, Vancouver, Canada.
- [25] "Human Induced Vibration of Steel Structures." HIVOSS, RFS2-CT-2007-00033
- [26] Rainieri, Carlo, Fabbrocino, Giovanni. "Operational Modal Analysis of Civil Engineering Structures, An Introduction and Guide for Applications." 2014
- [27] The Institute of Structural Engineers. "Structural Use of Glass in Buildings." SETO, London, 1999